Endothelio-Mesenchymal Interaction Controls *runx1* Expression and Modulates the *notch* Pathway to Initiate Aortic Hematopoiesis

Charlotte Richard,[1,4] Cécile Drevon,[1,4] Pierre-Yves Canto,[1] Gaelle Villain,[1] Karine Bollérot,[1] Aveline Lempereur,[1]
Marie-Aimée Teillet,[1] Christine Vincent,[1] Catalina Rosselló Castillo,[2] Miguel Torres,[2] Eileen Piwarzyk,[3] Nancy A. Speck,[3]
Michèle Souyri,[1] and Thierry Jaffredo[1,*]
[1]CNRS, UPMC, UMR7622, Bat C, 6ème étage, Case 24, 75252 Paris Cedex 05, France
[2]CNIC-Instituto de Salud Carlos III Melchor Fernández Almagro, 3 E-28029 Madrid, Spain
[3]Abramson Family Cancer Research Institute and Department of Cell and Developmental Biology, University of Pennsylvania School of
Medicine, Philadelphia, PA 19104, USA
[4]These authors contributed equally to this work
*Correspondence: thierry.jaffredo@upmc.fr
http://dx.doi.org/10.1016/j.devcel.2013.02.011

SUMMARY

Hematopoietic stem cells (HSCs) are produced by a small cohort of hemogenic endothelial cells (ECs) during development through the formation of intra-aortic hematopoietic cell (HC) clusters. The Runx1 transcription factor plays a key role in the EC-to-HC and -HSC transition. We show that Runx1 expression in hemogenic ECs and the subsequent initiation of HC formation are tightly controlled by the subaortic mesenchyme, although the mesenchyme is not a source of HCs. Runx1 and Notch signaling are involved in this process, with Notch signaling decreasing with time in HCs. Inhibiting Notch signaling readily increases HC production in mouse and chicken embryos. In the mouse, however, this increase is transient. Collectively, we show complementary roles of hemogenic ECs and mesenchymal compartments in triggering aortic hematopoiesis. The subaortic mesenchyme induces Runx1 expression in hemogenic-primed ECs and collaborates with Notch dynamics to control aortic hematopoiesis.

INTRODUCTION

In vertebrates, the aorta was shown to autonomously generate adult-type hematopoietic stem cells (HSCs) during development. Aortic hematopoiesis is characterized by the production of small clusters of hematopoietic cells (HCs) that accumulate in the lumen, closely associated with the endothelial floor (Dieterlen-Lièvre et al., 2006; Dzierzak and Speck, 2008). Polarization of hematopoiesis to the vessel floor in the avian embryo was shown to rely on the replacement of the initial aortic roof by somite-derived endothelial cells (ECs) (Pardanaud et al., 1996; Pouget et al., 2006). Polarization is under the control of a reciprocal Hedgehog-BMP molecular gradient in the zebrafish

embryo (Wilkinson et al., 2009) and/or activated by a somitic Wnt16/Notch pathway (Clements et al., 2011). In the mouse, HCs are found both dorsally and ventrally in the aorta (Taoudi and Medvinsky, 2007; Yokomizo and Dzierzak, 2010), but HSCs are restricted to the ventral side, suggesting that underlying tissues influence hematopoietic production (Taoudi and Medvinsky, 2007).

Compelling evidence indicates that HCs are derived from specialized ECs endowed with a hemogenic potential in the avian (Jaffredo et al., 1998), mouse (de Bruijn et al., 2000; Zovein et al., 2008), and human (Oberlin et al., 2002) embryos, although a subaortic origin cannot be completely ruled out (Bertrand et al., 2005; Rybtsov et al., 2011). Live-imaging techniques showed that embryonic stem cells generated ECs that, in turn, produced HCs (Eilken et al., 2009; Lancrin et al., 2009). Finally, time-lapse approaches showed that this production occurs in vivo in mouse aortic explants (Boisset et al., 2010) and in whole zebrafish embryos (Bertrand et al., 2010a; Kissa and Herbomel, 2010; Lam et al., 2010).

When and how the hemogenic program is induced are yet to be discovered. Several lines of evidence, however, indicate that local environmental signals influence hematopoiesis. For instance, an inductive/trophic effect of endoderm on mesoderm was shown to confer hemogenic potential to nonhemogenic ECs (Pardanaud and Dieterlen-Lièvre, 1999) or to influence HSC number in the aorta (Peeters et al., 2009). The presence of several molecules involved in hematopoiesis suggests that the ventral aortic mesenchyme may serve as a hematopoiesis-promoting microenvironment (Marshall et al., 2000). Moreover, cell lines isolated from the aortic region are potent supporters of embryonic and adult hematopoiesis (Oostendorp et al., 2002). However, the origin and role(s) of the subaortic mesenchyme are poorly understood. The problem lays primarily in the facts that (1) due to specific embryological constraints in the mouse embryo, endothelium and subaortic mesenchyme are not amenable to physical separation, and (2) both endothelium and subaortic mesenchyme are reported to express the key transcription factor Runx1, making the situation difficult to analyze (Azcoitia et al., 2005; North et al., 1999). Runx1 is responsible for the production of HCs and HSCs in the aorta

(North et al., 1999, 2002) and seems to be required for the earliest phases of HC formation from the endothelium but dispensable for the later ones (Chen et al., 2009). Yet neither the precise time point at which Runx1 is expressed during aortic hematopoiesis nor the developmental events controlling its expression have been identified.

Considering that aortic hematopoiesis mostly originates from hemogenic ECs, it can be viewed as a cell fate change in which ECs lose their characteristics and acquire hematopoietic-specific markers (Jaffredo et al., 2010). This endothelial-to-hematopoietic transition is under the control of the Notch pathway. Notch regulates cell fate decisions in many developmental systems including hematopoiesis. Gene inactivation experiments showed that Notch signaling and the Notch ligand Jagged1 are involved in embryonic hematopoiesis (Hadland et al., 2004; Kumano et al., 2003); Notch signaling activates Gata2 expression via RBPjκ (Robert-Moreno et al., 2005, 2008). The Notch pathway was shown to be upstream of the genetic cascade driving Runx1 expression during hematopoietic production in the zebrafish aorta (Burns et al., 2005) and be specifically required for HSC formation (Bertrand et al., 2010b; Rowlinson and Gering, 2010) through a Wnt16-dependant mechanism (Clements et al., 2011).

Here, we show that during aorta formation, Runx1 expression is a secondary event tightly controlled by the subaortic mesenchyme but that mesenchyme is not a source of HCs. Absence of the subaortic mesenchyme prevents both Runx1 expression and HC formation, showing the interdependent roles of the hemogenic EC and mesenchyme. However, the subaortic mesenchyme has no influence on vessel identity. Neither periaortic smooth muscle cells nor the mesonephros influenced aortic hematopoiesis. Runx1 expression is accompanied by downregulation of the Notch pathway in hemogenic ECs, a prerequisite to initiate hematopoiesis. This mechanism is conserved, but a few members of the Notch pathway display species-specific differences. Moreover, blocking Notch signaling results in overproduction of CD45$^+$ cells from the aorta. Taken together, our work opens the field for the future identification of critical regulators of aortic hematopoiesis and points to a necessary comparison between species for future biomedical applications.

RESULTS

Runx1 Expression Is Spatially and Temporally Controlled during Formation of the Aorta

We established the expression patterns of *runx1*, *pu-1* (a Runx1 target; Huang et al., 2008), and *c-myb* (a Runx1 molecular partner; Hernandez-Munain and Krangel, 1994) by in situ hybridization on adjacent sections at selected stages of aorta formation in the chick embryo. Expression was examined at stages representing prefusion paired aortas, and postfusion aortas before the HC stage, at 48 hr (Figures 1A and 1A′; Figures S1A–S1D available online), 55 hr (Figures 1B and 1B′), and 60 hr (Figures 1C, 1C′, and S1E–S1J) of development. Later stages displayed already-reported *runx1* expressions in the hemogenic endothelium and the hematopoietic clusters and were not included in the figures. *Runx1* expression was found to initiate in the lateral aspect of the paired aortas 1 day before

the HC stage and to progressively extend ventrally while remaining confined to the endothelial layer marking the hemogenic endothelium. *Pu-1* and *c-myb* mRNAs followed *runx1* expression with a slight delay and also marked the hemogenic endothelium (Figures S1A–S1J) and HCs (data not shown). Contrary to the mouse expression pattern (Azcoitia et al., 2005; North et al., 1999; Zovein et al., 2008), no *runx1* mesenchymal expression was found in the chicken embryo. This lateral-to-ventral pattern strongly suggested that *runx1* expression was tightly controlled. We thus sought tissues or cells whose association or migration to the floor of the aorta was contemporaneous with *runx1* expression.

Mapping the Origin of the Subaortic Mesenchyme

We focused on the subaortic mesenchyme, whose onset of formation and subsequent differentiation were coincident with *runx1* expression pattern. Subaortic mesenchyme was recently shown to originate from the lateral plate mesoderm in mouse (Wasteson et al., 2008) and chicken embryos (Wiegreffe et al., 2009), but the precise location of the mesenchymal precursors was not defined. Based on the observation of E1.5–E2 avian embryos, a splanchnopleural origin appeared likely.

We performed fate-mapping experiments using DiI labeling and quail/chicken grafts. In the first series of experiments, groups of cells in 10–13 somite-stage embryos were labeled using DiI crystals that were inserted in the splanchnic mesoderm at the level of the last-formed somite, at different distances from the midline (n = 22; Figures 1D and 1E). Six samples, recorded during 24 or 36 hr, showed very dynamic movements (Movie S1). DiI$^+$ cells that were lateral to the somites moved to the embryo midline. This movement is due to the formation of the lateral body folds that raises the embryo body and, at the same time, allows left and right splanchnic epithelial sheets to meet. Distance measurements showed that DiI$^+$ cells moved at a constant speed of 11 μm/hr, covering about 300 μm to reach the midline (Figure 1F; Movie S1). Analysis of sections showed that DiI$^+$ cells localized underneath the aorta (Figure 1G) and never crossed the midline. In most cases, ECs were not labeled. Placing the crystals more superficially, immediately underneath the endoderm, resulted in aortic endothelium staining (Figure 1H), demonstrating the close association between the splanchnic mesoderm and aortic rudiments and the ventral origin of the primitive aorta. In a second series of experiments, pieces of chicken splanchnic mesoderm were replaced by their quail counterparts (17 embryos), and the location of quail cells was monitored with the quail-specific antibody QCPN (data not shown). DiI and quail-chicken approaches yielded similar results. These approaches were completed with scanning electron microscopy studies or normal embryos during E2. In Figure S1K (22 somite-stage embryo), the splanchnic epithelium began to wrap around the aortic rudiment. Slightly later on, cells reached the aortic floor (Figure S1L).

In conclusion, the subaortic tissue originated from a splanchnic mesoderm segment localized between 250 and 300 μm from the embryo midline. Labeled cells lateral to this segment associated with the future gut (data not shown), revealing a precise dorsoventral allocation of splanchnic mesodermal blocks according to their medio-lateral position.
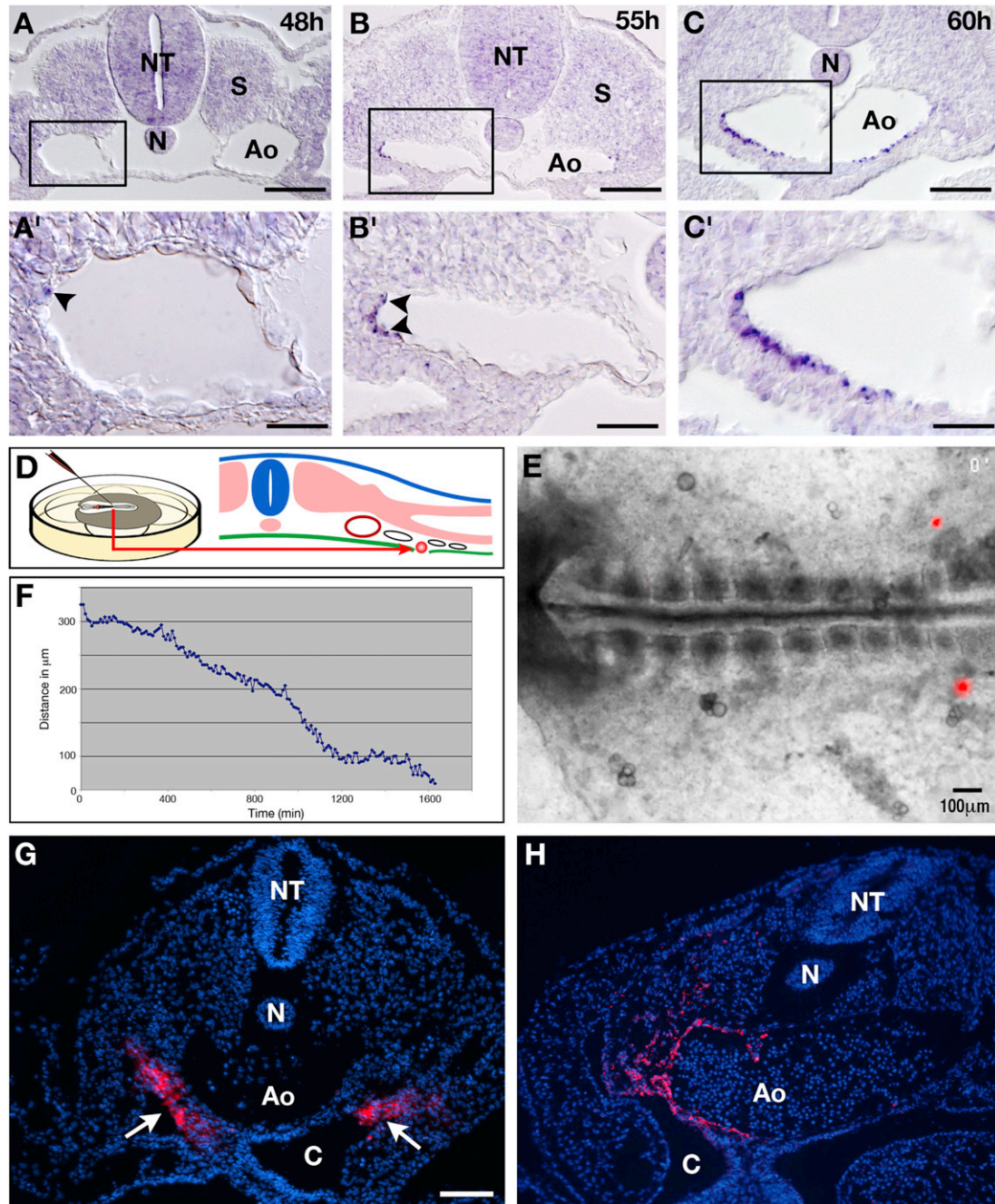
Figure 1. Runx1 Patterns and Dynamics of Aorta Formation

(A–C′) Aortic *runx1* expression. In situ hybridization. (A) Early-paired aortae stage; 48 hr. No conspicuous *runx1* expression is present at that stage. Scale bar, 50 μm. (A′) Magnification of the frame in (A). A single *runx1*[+] cell is present in the lateral endothelium (arrowhead). Scale bar, 15 μm. (B) Late-paired aortae stage; 55 hr. *Runx1* is barely detectable. Scale bar, 70 μm. (B′) Higher magnification of the frame in (B). *Runx1* expression is restricted to a few cells in the ventrolateral endothelium (arrowheads). Scale bar, 20 μm. (C) Single-aorta stage, immediately after fusion; 60 hr. *Runx1* is expressed throughout the whole ventral endothelium except in its ventral most part. Scale bar, 80 μm. (C′) Magnification of the frame in (C) showing the endothelial-specific expression of *runx1*. Frames focus on the left side of the aorta that are higher magnified in corresponding (A′)–(C′). Scale bar, 25 μm.

(D–G) Fate mapping of the subaortic mesenchyme. (D) Experimental design. The embryo is cultured ventral side up. Endoderm is opened, and a DiI crystal (red arrow) is deposited on the splanchnopleural mesoderm. (E) Ten somite stage. Bilateral deposition of crystals visible as red spots. (F) Speed measure of a DiI crystal. Crystal progression is constant over time. (G) Cross-section through a 12 somite-stage embryo bilaterally labeled with DiI after 24 hr of culture. The DiI[+] areas are immediately underneath the aorta (white arrow). Scale bar, 70 μm.

(H) Splanchnopleural origin of the primitive aorta. In addition to the splanchnopleural mesoderm, the aorta was sometimes labeled indicating that both tissues have the same origin. Here, a single DiI crystal was deposited on one side resulting in the staining of the whole hemiaorta and associated mesenchyme.

Ao, aorta; C, coelom; N, notochord; NT, neural tube; S, somite. See also Figure S1 and Movie S1.

Preventing Migration of the Subaortic Mesenchyme Inhibits Runx1 Expression and Initiation of Hematopoiesis without Impairing Vessel Formation or Arteriovenous Identity

Fate-mapping experiments prompted us to study the role of the subaortic mesenchyme in the initiation of hematopoiesis. Migration of mesenchyme to the midline was prevented by making a slit on one side of the embryo, either immediately lateral to the somite or in the intermediate mesoderm, that separated the embryo proper from the lateral plate (Figure 2A). The nonoperated side served as control. Both experiments yielded similar results. The slit was made at E2 when the embryo was still flat and no contact between lateral plate and aortic anlagen had yet occurred (Figure 2A). The slit does not modify the dorsoventral allocation of hemogenic and nonhemogenic ECs of the aorta because (1) it was made when the aortic anlagen was still formed, and (2) the global shape of the aorta and the presence and correct position of the segmental arteries, derived from the somite, are not modified. Lack of lateral plate resulted in the absence of a coelom, fusion between ectoderm and endoderm, and formation of a hemidigestive tube on the operated side (Figure 2B). One day after the slit was made, the paired aortas fused, but no conspicuous sign of aortic hematopoiesis was yet visible (n = 3). *Runx1* was expressed by ventral aortic ECs on the control side but was totally absent on the operated side (Figure 2C). *Vascular endothelial* (*ve*) *cadherin* was expressed normally, showing that vascular EC identity was not impaired by the operation (Figure 2D). *Delta-like4* expression was maintained, demonstrating no change in arteriovenous identity (Figure S2A). Two days after the slit was made, *runx1*⁺ HCs were visible in the control, but not in the operated side (Figure 2E) (n = 4), consistent with the lack of runx1 endothelial expression 1 day earlier. *Ve*-cadherin remained expressed by ECs, but its expression on the control side was downregulated in HCs (Figure 2F), in keeping with our previous data (Jaffredo et al., 2005). *Delta-like4* was also maintained in ECs and downregulated in HCs (Figure S2B). Formation of the subaortic mesenchyme thus appeared critical for the initiation of *runx1* expression and the production of HCs. However, the absence of mesenchyme had no influence on the expression of arterial markers, indicating that the lack of *runx1* expression and the absence of HCs on the operated side were not due to a loss of arterial identity.

We used the same experimental approach to analyze the role of smooth muscle cells in the initiation and maintenance of aortic hematopoiesis. No difference was seen in smooth muscle actin expression in the control and operated sides (Figure S2C), demonstrating that this tissue is not sufficient by itself to induce *runx1* expression and cluster formation in the absence of subaortic mesenchyme. Finally, because a role for mesonephros and Wolffian duct had been suggested, we selectively removed the intermediate mesoderm over the length of four somites on one side, with the nonoperated side serving as the control. In addition to morphological criteria, *cjagged2* was used to confirm the absence of mesonephros. One day after the ablation, *runx1* was found in both the operated and nonoperated sides, indicating that signaling from the mesonephros is not required for hematopoietic specification (Figure S2D and S2E).
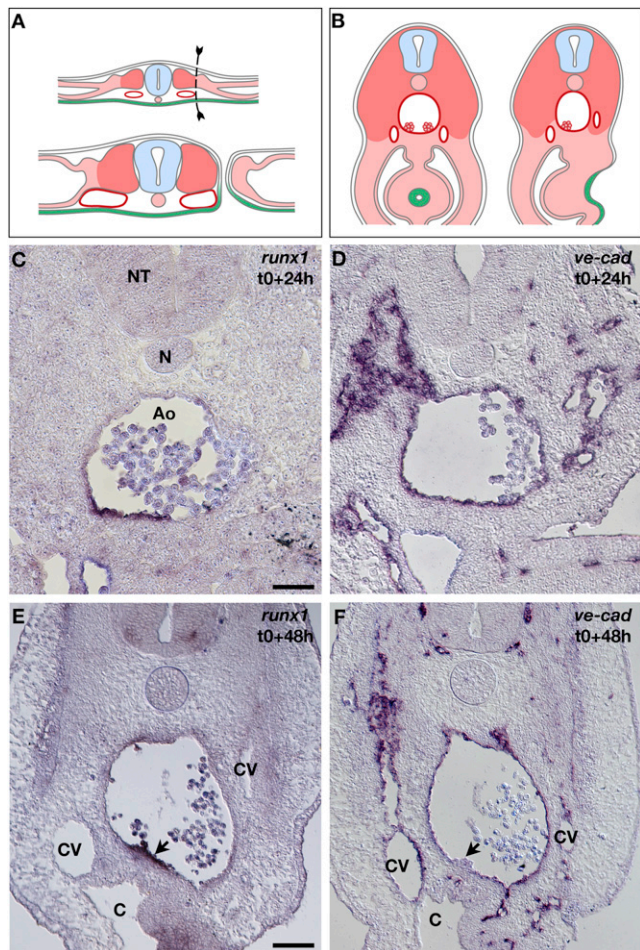

Figure 2. Role of the Subaortic Mesenchyme in Aortic Hematopoiesis

(A) Experimental scheme and further development. The cut separates somite and future kidney from the lateral plate (upper scheme), preventing the splanchnopleural mesoderm to contribute to the aortic region (lower scheme). Ectoderm is shown in white, endoderm in green, somites in dark pink, and lateral plate in light pink.

(B) Schematic representation of normal and operated embryos 48 hr after the slit. Midtrunk level. Left-hand scheme shows normal embryo. Somite-derived structures are in dark pink. The aorta (red, median circle) has two rows of HCs. The gut composed of endoderm (green) surrounded by mesenchyme (light pink) is appended into the coelomic cavity. Right-hand scheme illustrates operated embryo. Symmetry is not affected except in the ventral part of the embryo. Aortic hematopoiesis pattern is affected. Coelom on the operated side is lacking, and gut is opened. Endoderm and ectoderm have fused.

(C–F) Aortic region at 24 hr (C and D) and 48 hr (E and F) after the slit. In situ hybridization with *runx1* (C and E) and *ve-cadherin* (D and F). (C) *Runx1* expression is present on the control side (left) but absent on the operated side (right). Scale bar, 130 μm. (D) *ve-cadherin* pattern is normal suggesting that no major modification of EC identity has occurred. (E) *Runx1*⁺ HC clusters are visible on the control side (black arrow) but are lacking on the operated side. Note the presence of a loose ventral tissue on the operated side compared to the control side. Scale bar, 150 μm. (F) *ve-cadherin* expression is normal. Note the decrease of *ve-cadherin* expression mRNA in the HC clusters as reported (Jaffredo et al., 2005). Black arrow points to a HC cluster.
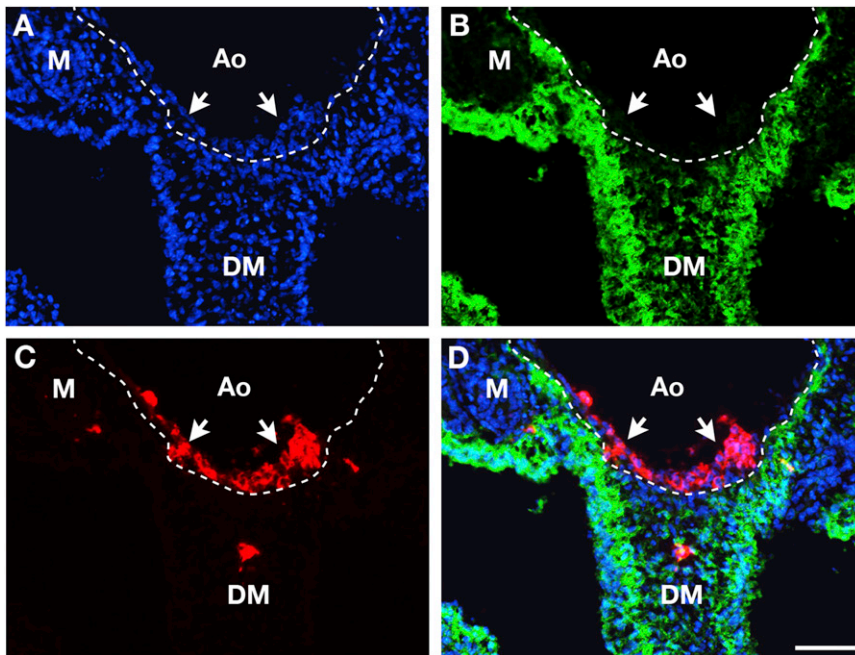
C, coelom; CV, cardinal vein. See also Figure S2.

Figure 3. Tracing Splanchnopleural Mesoderm Derivatives Using CFDA-SE

(A–C) Twenty-four hours after CFDA-SE labeling. Same section triple stained with DAPI (A), CFDA-SE (B), and CD45 (C). The dotted line indicates the limit between the endothelium and the subaortic mesenchyme. DAPI staining reveals the topography of the tissues. CFDA-SE stains the subaortic mesenchyme and the coelomic epithelium. CD45 stains the aortic clusters (white arrows).

(D) Merge of DAPI, CFDA-SE, and CD45 signals. The aortic HC clusters were never green, in keeping with an endothelial origin of HC clusters and the complementary roles of aortic endothelium and subaortic mesenchyme in aortic hematopoiesis. Scale bar, 80 μm.

DM, dorsal mesentery (of splanchnopleural origin); M, mesonephros.

Endothelial, but Not Mesenchymal, Origin of the Hematopoietic Clusters

The absence of HCs following the block of subaortic mesenchyme migration could be due to either a lack of induction on the hemogenic endothelium or an absence of HCs carried by the mesenchyme. To discriminate between these possibilities, we labeled the whole lateral plate mesoderm at the epithelial stage with the lipophilic dye 5-(and-6)-carboxyfluorescein diacetate, succinimidyl ester (CFDA-SE) and followed the labeled cells until the HC stage. Because the splanchnic epithelium gives rise to the subaortic mesenchyme, we expected the mesenchyme to be fluorescent. If HCs originate from this source, they should also be labeled. CFDA-SE was inoculated into the coelom, allowing cells lining the cavity to be labeled. Two-day embryos received 1–2 μl of 5 μM CFDA-SE and were further incubated for 24 hr. Seven embryos were analyzed; all displayed a similar staining. The subaortic mesenchymal cells were CFSE$^+$ (Figures 3A and 3B), but CD45$^+$ HC clusters were free of CFSE labeling (Figures 3C and 3D), indicating that they did not originate from the subaortic mesenchyme.

Interplay between Notch Signaling and Runx1 Expression in Aortic Hematopoiesis

We investigated the role of Notch signaling during the early steps of aortic hematopoiesis. *Serrate1* and *serrate2* are avian orthologs of mouse Notch ligands *Jag1* and *Jag2* (and will hereafter be referred to as cjagged1 and 2, respectively). Both *cjagged1* and *cjagged2* displayed the same expression pattern by in situ hybridization during aortic development (data not shown), but because *cjagged2* yielded the better signal, it was chosen for further analysis. At the 29–32 somite stage, the time of aortic fusion for the level considered, *cjagged2* was present throughout all aortic ECs (Figure S3B), and *runx1* expression intensified (Figure S3A). Immediately after fusion, *cjagged2* expression decreased in the two ventral ridges (Figure 4B) where *runx1* dis-

played the strongest expression (Figure 4A). At the cluster stage, *cjagged2* and *runx1* became mutually exclusive (Figures S3C and S3D). Thus, *runx1* expression is associated with downregulation of the *cjagged1* and *cjagged2* Notch ligands, which become restricted to ECs.

qPCR Analysis Demonstrates Downregulation of the Notch Pathway during Aortic Hematopoiesis

Avian and mouse embryos at pre-HC (E2.5 and E9) and HC (E3.5 and E11.5) stages were used to isolate ECs and HCs from the aortic region by flow cytometry, and expression of members of the Notch pathway and several Notch targets was probed by qPCR (Supplemental Experimental Procedures; Table S1). Both avian and mouse embryos displayed a similar expression pattern of Notch signaling in ECs at the pre-HC stage (Figures S3E and S3F). Expression of several Notch pathway members, including *Jag2*, *Dll4*, and *Gata2*, was enriched in the EC fraction compared to the nonendothelial fraction, whereas *Notch1*, *Jagged1*, *RbpjK*, *Hes1*, and *Hey2* displayed weaker levels of expression relative to the non-EC fraction (Figures S3E and S3F). The EC-associated expression pattern remained unchanged at the time of HC production, but there was a strong decrease in Notch ligand expression (*Jag1*, *Jag2*, *Dll4*) and an increase in *RbpjK* expression in the HC as compared to the EC population (Figures 4C and 4D). Although changes were more visible in the chicken embryo, both species followed the same pattern, except for *Jag2* in the mouse embryo, which showed no decrease in HCs relative to ECs (Figure 4D).

We also took advantage of the Runx1-GFP reporter mouse (Lorsbach et al., 2004) to analyze expression of the Notch target *Hes1* in a purified population of hemogenic endothelium (Runx1-GFP$^+$CD144$^+$CD41$^-$CD45$^-$), an immature HC population (Runx1-GFP$^+$CD144$^+$CD41$^+$CD45$^-$), and two more mature HC populations (Runx1-GFP$^+$CD144$^+$CD41$^+$CD45$^+$ and Runx1-GFP$^+$CD144$^+$CD41$^-$CD45$^+$) at the 40–45 somite pair stage (E11.5). All three HC populations had a reduced level of *Hes1* expression relative to ECs (Figure 4E). Together, the data suggest that Notch signaling is reduced in HCs relative to hemogenic ECs.

Active Notch1 Is Expressed by Both the Aortic Endothelium and the Subaortic Mesenchyme

As another approach to identify cells in the aortic region that contained activated Notch, we electroporated the Notch reporter plasmid pTP1-Venus (Kohyama et al., 2005) into the chick aorta (Rosselló and Torres, 2010). We found GFP$^+$ cells both in the endothelium (Figure S3G) and in the subaortic mesenchyme (Figure S3H) before the HC stage. However, during the HC stage, Notch signaling remained present in ECs and in tissues surrounding the aorta but disappeared from the HCs (Figures 4F and 4G) (n = 15). In situ hybridization and immunohistochemistry demonstrated the presence of Notch1, but not Notch2, in the aortic region (data not shown), suggesting that the active Notch signal was derived from Notch1.

Blocking γ-Secretase Activity Promotes Hematopoietic Production in Aorta Organotypic Culture and Whole-Embryo Culture

In order to evaluate the role of Notch signaling in aortic hematopoiesis, we employed the widely used chemical Notch inhibitor, DAPT, to block γ-secretase activity and prevent cleavage of the Notch intracellular domain. We added 50 μM DAPT to E9.5 (20–25 somite pairs) mouse P-Sp explant cultures. No significant difference in cell counts was found between control and DAPT-treated cultures after 7 days (four independent experiments in the mouse; Figure 4H). We first examined the production of CD45$^+$ HCs (which includes both committed HCs and progenitors) after 3 and 6 days. Three days after DAPT treatment, mouse P-Sp explants contained significantly more CD45$^+$ cells compared to vehicle-treated controls (Figure 4I), suggesting that the downregulation of Notch signaling that accompanies HC cluster formation augments HC production. After 6 days of explant culture, the inverse is observed (Figure 4J), indicating that the enhancing effect of DAPT on CD45$^+$ cell number was transient. We checked whether this could be related to an increase of apoptosis or cell death during the culture. Flow cytometric analysis of the CD45$^+$ fraction with annexin V and 7AAD revealed that DAPT treatment did not alter the percentage of 7AAD$^+$ cells in the CD45$^+$ population of mouse AGM explant cultures at either 3 or 6 days (Figure 4K). In contrast, during this time course, the percentage of apoptotic annexin V$^+$ 7AAD$^-$ cells increased more in the DAPT-treated cultures than in controls (2- versus 1.7-fold; data not shown). Thus, differences in the initial phases of CD45$^+$ HC production and response of HC to apoptosis and cell death explain the differential effects of DAPT treatment at early and late time points in the explant culture period. We next quantified the number of hematopoietic progenitors after 7 days of explant culture with or without 50 μM DAPT. Clonogenic progenitors were assayed in methylcellulose and in day 7-cobblestone area-forming cell (D7-CAFC) assays. Mouse D7-CAFCs, as well as total CFCs (data not shown), were decreased 2- to 3-fold (p = 0.05) in the presence of DAPT (Figure 4L), in keeping with previous data by Robert-Moreno et al. (2008), and consistent with the DAPT-induced decrease in CD45$^+$ cells after 6 days of explant culture.

When chicken P-Sps at equivalent hematopoietic stages (26–30 somite pairs) were treated in the same conditions, no significant difference in cell counts was found between control and DAPT-treated cultures after 7 days (five independent experiments; Figure S3I). However, CD45$^+$ HCs produced in DAPT-treated samples were found to be less sensitive to cell death than their nontreated counterpart (Figure S3J). Again, hematopoietic progenitors were also quantified. Because not all hematopoietic cytokines for chick progenitors are commercially available, only D7-CAFC assays were performed for chick aorta cells by coculturing with MS5 stromal cells. In contrast to the mouse, the number of D7-CAFCs was increased in chick cultures in the presence of DAPT (p = 0.016; Figures S3K and S3L). We also exposed whole chicken embryos to DAPT and examined CD45$^+$ cells in the aorta. DAPT was delivered to the endoderm, close to the aortic anlagen. Treatment was performed at the 29–32 somite stage and lasted 24 hr (n = 6). Application at earlier stages resulted in abnormalities and death. DMSO caused hemorrhages in the yolk sac but did not impair embryo viability (Figure 5A). Sections revealed a large increase in the number of CD45$^+$ cells after 24 hr of DAPT exposure, in keeping with the increase seen in short-term mouse P-Sps explant cultures. In the most dramatic cases, the aorta was filled with CD45$^+$ cells that formed a giant cluster (Figures 5B and 5C). In some instances, we found some dorsal ECs expressing CD45, but the majority of the CD45$^+$ cells remained attached to the ventral side. No HC cluster was detected in the cardinal veins, indicating that DAPT treatment did not change the identity of the vessels, as confirmed by the artery-specific marker *delta-like4* (data not shown). We occasionally observed CD45$^+$ HC clusters in the paired aorta (Figure 5D), which was never seen in vehicle-treated embryos, indicating that hematopoietic production was also accelerated. We believe that the difference in the response of chick and mouse HCs to DAPT is due to (1) a DAPT-induced increase of apoptosis at 6 days of culture, leading to a decrease in CD45$^+$ cells in the mouse culture, and (2) a lower sensitivity to cell death of chick HCs produced in DAPT-treated samples compared to their nontreated counterpart.

DISCUSSION

Our study unravels the critical role of the subaortic mesenchyme in regulating Runx1 expression in the hemogenic endothelium and the role of the associated Notch pathway in these early events. Conserved Runx1 regulatory elements from chicken to human suggested common regulatory pathways between species (Bee et al., 2009; Ng et al., 2010; Nottingham et al., 2007). Despite these insights, it was not clear whether Runx1 was constitutively expressed from the onset of aorta formation or secondarily regulated by developmental events. Here, we show that ECs of the aortic anlage did not express *runx1* nor *pu1* and *c-myb*. Instead, *runx1* and associated genes are secondarily expressed as aortas matured. In addition, *pu1* and *c-myb* mRNAs are found expressed in the hemogenic endothelium earlier than expected, further documenting the EC-to-HC switch.

Before the present study, the subaortic tissue was thought to originate from the lateral plate mesoderm (Wasteson et al., 2008; Wiegreffe et al., 2009). Using tracing techniques, we identified a band of splanchnic mesoderm giving rise to the subaortic tissue; cells lateral to this band contribute to the gut mesoderm revealing a specific allocation of splanchnopleural
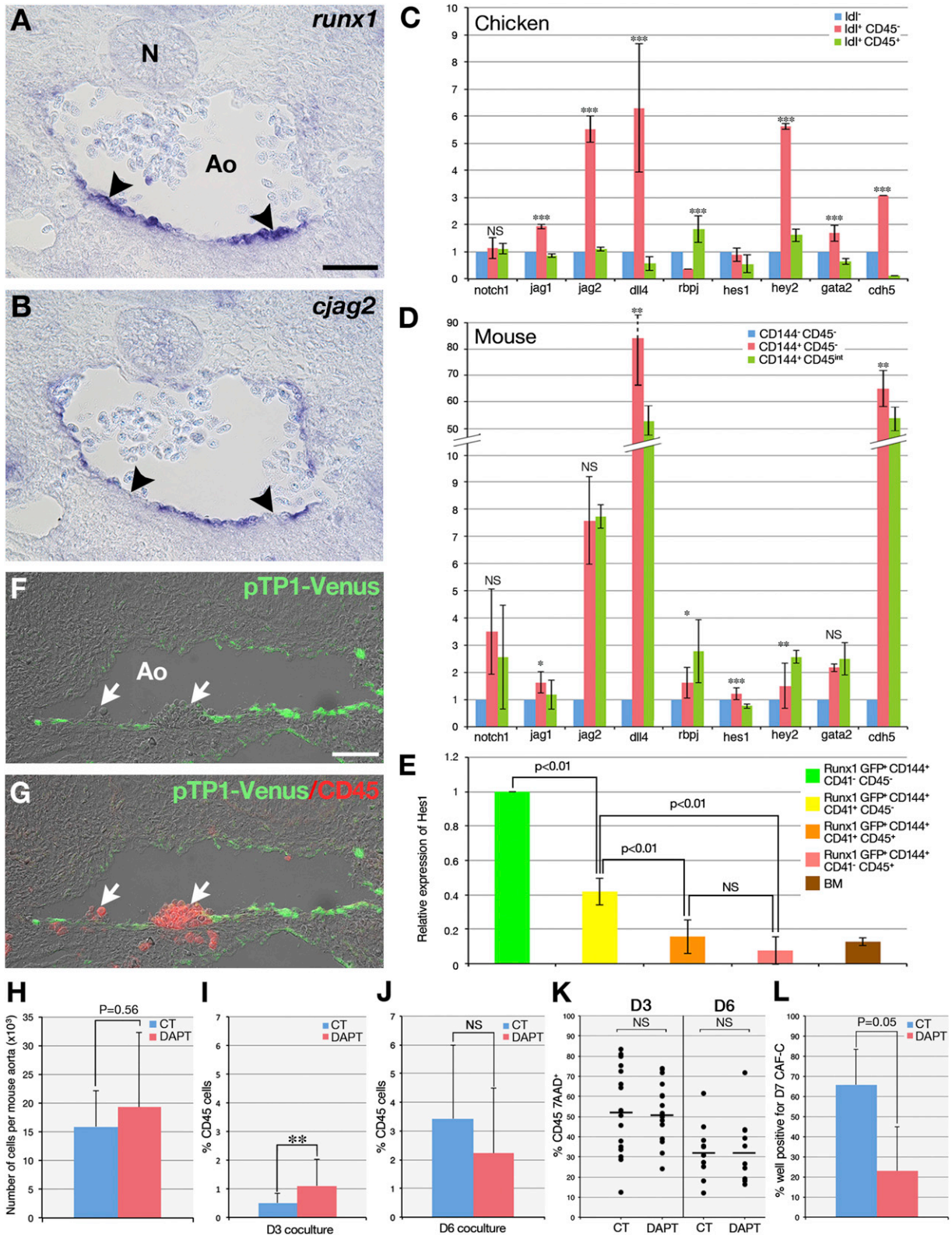
Figure 4. Analysis of the Notch Pathway during Aortic Hematopoiesis

(A and B) Mutual exclusion between *cjagged2* and *runx1* during aortic hematopoiesis. In situ hybridization, adjacent sections separated by 7 μm. (A) *Runx1* expression extends to the whole floor (arrowheads) except to ECs in the midline. Scale bar, 150 μm. (B) *Cjagged2* expression is lost (arrowheads) in cells upregulating *runx1*.

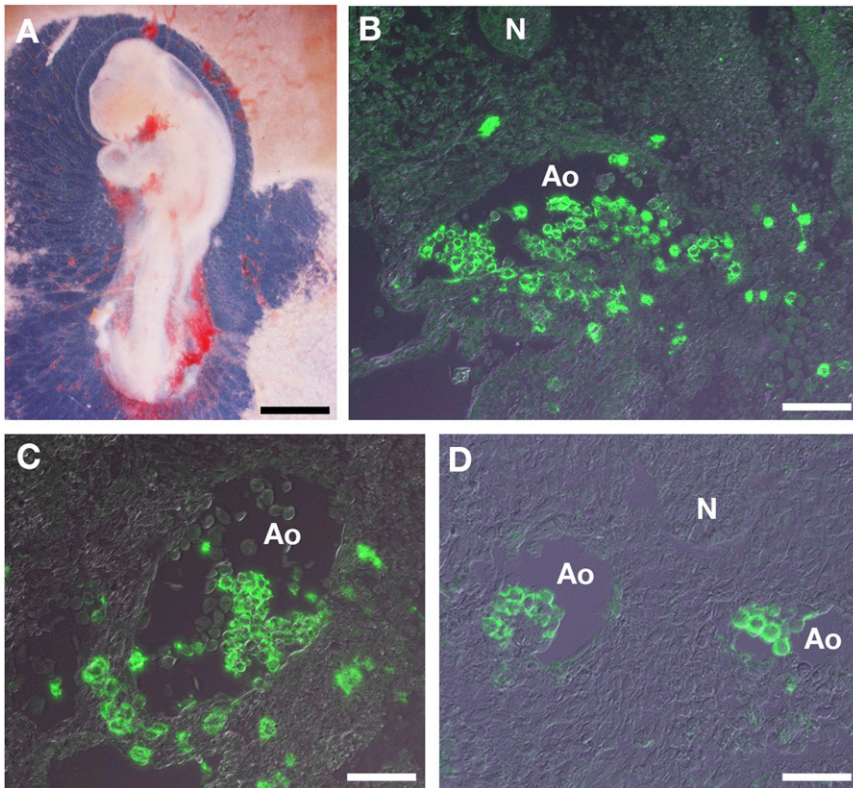*(legend continued on next page)*

Figure 5. Effect of Whole-Embryo DAPT Treatment on Aortic Hematopoiesis

(A) Representative embryo following DAPT treatment. No gross anomaly is visible, but some blood lacunae have formed. Scale bar, 1 mm.

(B and C) Cross-sections through the aorta of a treated embryo after 24 hr. CD45 immunohistology. Numerous CD45$^+$ cells are present in the aortic lumen. These structures form a large HC cluster attached to the ventral aortic side. Scale bar, 50 μm.

(D) Ectopic hematopoiesis in the paired aortae. A ventral HC cluster on the left-hand aorta and a dorsal cluster on the right-hand aorta are clearly visible. HCs are never seen at this level in normal embryos. Scale bar, 50 μm.

cells along the medio-lateral axis. The tracing techniques also demonstrate the initial splanchnopleural-associated origin of the aortic rudiments.

The experimental block in the migration of the subaortic mesenchyme demonstrates the critical role of this tissue for *runx1* expression and aortic hematopoiesis. Whether the mesenchyme is required for the initiation or also for further hematopoietic steps needs to be determined. Our data also suggest that the splanchnopleure-derived aortic hemogenic endothelium is primed to express *runx1* but does not express it because it receives signal(s) from the mesenchyme that triggers the hematopoietic program. A supportive role for the subaortic mesenchyme has been proposed several years ago, but never experimentally demonstrated, based on the presence

of TGF-β family molecules and tenascin, known to be key factors in hematopoietic development, thus constituting the earliest HSC niche (Cortés et al., 1999; Marshall et al., 2000; Marshall et al., 1999). Cell lines derived from this region exhibit a strong hematopoietic support and are phenotypically characterized as stromal cells (Durand et al., 2007; Oostendorp et al., 2002). BMP4 is present in the subaortic mesenchyme and plays a prominent role in promoting HSC survival and expansion (Durand et al., 2007). In zebrafish, subaortic BMP would trigger *runx1* expression in the ventral aspect of the aorta (Wilkinson et al., 2009). Although we have not specifically addressed the molecular nature of the initiating signal, submesenchymal BMP4 is clearly present in the avian embryo at the time of hematopoietic emergence and may play a role in *runx1* induction. In the mouse embryo, the positive role of BMP appears to be precisely regulated by inhibitory Smads (Pimanda et al., 2007). However, BMP signaling, testified by the expression of the phosphorylated Smads 1, 5, and 8, is present from the earliest phases of chicken aorta formation before *runx1* becomes expressed (C.R., C.D., and T.J., unpublished data). Thus, if BMP4 is necessary for *runx1* induction, it does not appear to be sufficient to trigger *runx1* expression,

(C and D) qPCR analysis of the Notch pathway in AGM ECs at the hematopoietic stage in chicken (C) and mouse (D) embryos, i.e., E3.5 and E11.5, respectively. ECs (pink) were sorted on the basis of AcLDL uptake (chicken) and CD144 expression (mouse). HCs (green) were retrieved by including the expression of CD45.

(E) Hes1 expression analysis by qPCR in the E11.5 Runx1$^+$ hemogenic endothelium compared to increasing stages of hematopoietic maturation characterized by their combinatorial expression of CD41 and CD45. A decrease in Hes1 expression associated with HC maturation from the endothelium is clearly visible.

(F and G) Detection of active Notch following pTP1-Venus reporter construct electroporation in the aorta. (F) HC cluster stage. Two clusters are visible (white arrows). The green staining (active Notch) is restricted to ECs and absent from the clusters. Scale bar, 40 μm. (G) Same section double stained for active Notch (green) and CD45 (red) to visualize the clusters.

(H–L) Hematopoietic production analysis of E9.5 mouse P-Sps treated or not with DAPT. (H) Number of cells in vehicle- and DAPT-treated aortas after 7 days of coculture on OP9 layer. Differences in cell number are not significant. (I and J) Percentages of CD45$^+$ cells produced by E9.5 mouse P-Sp after 3 (I) and 6 (J) days of culture with or without DAPT. A significant increase of CD45$^+$ cell production is visible at 3 days in the DAPT-treated samples compared to the vehicle-treated samples. The inverse is observed at 6 days of culture. Error bars represent the results from four independent assays. (K) Percentage of 7AAD$^+$ cells at 3 (D3) and 6 (D6) days following mouse P-Sp culture incipience. (L) Percentage of wells positive for D7-CAFCs. A significant decrease in CAFCs is observed in the DAPT-treated samples, in keeping with previously published data by Robert-Moreno et al. (2008).

The error bars represent SEM. ***p < 0.01, **p < 0.25, *p < 0.5. NS, not significant. See also Figure S3 and Table S1.

and additional signals are required. In these "slitted" embryos, peri-aortic smooth muscle cells appear normal, suggesting that this cell type is not involved in aortic hematopoiesis as previously proposed by Galmiche et al. (1993). This is also the case for the intermediate mesoderm derivative, the absence of which has no role in *runx1* expression.

Despite convincing reports on the central role of the aortic endothelium in generating hematopoiesis (Bertrand et al., 2010a; Boisset et al., 2010; Kissa and Herbomel, 2010; Lam et al., 2010), it was not clear whether the subaortic mesenchyme was also able to generate aortic clusters as proposed by Bertrand et al. (2005). CFDA-SE labeling demonstrates that HC clusters originate exclusively from the endothelium, whereas the subaortic mesenchyme is a hematopoietic-supportive tissue that does not produce HC, hence demonstrating the complementary roles of these two aortic compartments. This approach has also been successfully used to study the formation of aortic vascular smooth muscle cells (Wiegreffe et al., 2009).

Notch expression in aortic ECs and HCs displays a conserved signature between species. HC cluster production is accompanied by the decrease of Notch ligands. This pattern is, however, more prominent in the chicken embryo than in the mouse embryo and takes place as early as *runx1* expression initiates in the hemogenic endothelium. This pattern is also prominent as HCs mature from CD41$^+$ to CD45$^+$ cells. Our functional experiments also indicate that *notch1* signaling is downregulated in HC clusters. During the early phases of endothelio-mesenchymal interactions, *notch1* is, however, not expressed or expressed at low levels in the mesenchyme. Ligand expression being restricted to ECs, this pattern suggests a notch-independent mechanism of action. A requirement for Notch signaling and intraembryonic HSC production has been shown for mouse and zebrafish embryos. Loss-of-function experiments demonstrate that ablating Notch signaling suppresses definitive (embryo-derived), but not primitive (yolk sac-derived), hematopoiesis (Burns et al., 2005; Kumano et al., 2003; Robert-Moreno et al., 2005, 2008). Of note, in the mouse embryo, Notch1 and Jag1 are required for aortic hematopoiesis to occur (Robert-Moreno et al., 2008). Here, we show that suppression of Notch signaling enhances the production of CD45$^+$ HCs in mouse and chicken P-Sps. However, this production is transient, and 6 days after DAPT exposure, mouse P-Sp CD45$^+$ cells are less numerous in the DAPT-treated samples than in the vehicle-treated sample. Moreover, chicken CD45$^+$ HCs appear less sensitive to cell death when treated by DAPT. In keeping with HC production, CAFC formation in the mouse aorta is strongly reduced in the mouse P-Sp treated by DAPT as previously reported by Kumano et al. (2003) and Robert-Moreno et al. (2008) but is enhanced in chicken P-Sps. This in vitro effect is corroborated by the in vivo effect of DAPT on chicken embryos. We thus shed light on the apparent blockade of aorta hematopoiesis in the mouse embryo following Notch loss of function. Consistent with previous results by Burns et al. (2005) and Robert-Moreno et al. (2008), manipulating the hematopoietic production in the aorta using the Notch pathway has no effect on arterial identity because overproduction of HC clusters remains restricted to the aorta. Downregulation of Notch signaling in the hemogenic endothelium is thus required for aortic hematopoiesis to occur. Taken together, our study clearly pleads for a thorough comparison between models, especially if one aims at exploiting discoveries for future biomedical applications.

EXPERIMENTAL PROCEDURES

Embryos

Chicken (*Gallus gallus* JA57 strain) and quail (*Coturnix coturnix japonica*) eggs were incubated at 38°C ± 1°C in humidified atmosphere until embryos reached the appropriate stage. Embryos were either operated in ovo or cultured according to Chapman et al. (2001) and incubated at 37°C/5% CO$_2$.

Pregnant C57Bl6 mice were purchased from Janvier (France). Females were killed by cervical dislocation. Experiments were carried out in accordance with the guidelines of the French Veterinary Department. Approval was obtained from the French Ministry of Agriculture institutional review board for these studies.

Quail-Chicken Transplantations

Quail donor splanchnopleural mesoderm posterior to the last-formed somite was isolated and transplanted into chicken recipients of the same stage (10–13 somite) either in ovo or in culture. In ovo grafts were introduced throughout ectoderm and somatopleural layers into the splanchnopleural layer. In culture, grafts were inserted into a cut of approximately the same size performed ventrally. Grafted embryos were incubated for an additional 24–48 hr. Samples were fixed in 3.7% formaldehyde for 1 hr at room temperature (RT), embedded in paraffin, and processed for histochemistry.

In Ovo "Slits"

A total of ten embryos ranging from 13 to 17 somite pairs received India ink (Pelikan)/PBS solution (50:50) into the subgerminal cavity for visualization. A cut encompassing ten somites and passing through the three germ layers was made with a microscalpel. The slit lined either immediately lateral to the paraxial mesoderm or the intermediate mesoderm including the mesonephros in that latter case. Embryos were sacrificed 24–48 hr later.

Chicken Embryo Cultures and DAPT Treatment

Ten somite-stage embryos were washed in saline and transferred ventral side up onto a 35 mm dish according to Chapman et al. (2001). A drop of DAPT, N-(3,5-difluorophenylacetyl-L-alanyl)-S-phenylglycine t-ButylEster (InSolution γ-Secretase Inhibitor IX; Calbiochem), at 2.5 mM in DMSO was applied to the embryonic endoderm. Embryos were placed back in culture for 24 hr.

Labeling of the Splanchnopleural Mesoderm

Crystals of carbocyanine dye DiI were prepared according to Kimura et al. (2006). After local endoderm removal, DiI crystals of 5–30 μm in diameter were deposited with a glass micropipette onto the splanchnopleural mesoderm lateral to the last-formed somite. Labeled embryos were incubated, photographed, and processed for histology.

Image Acquisition

Chicken embryos were cultured ventral side up in dishes with a glass bottom in a humidified atmosphere at 37.5°C. They were observed under an inverted microscope (Leica; DMIRBE) with a 5× objective. Images were taken overnight using a CoolSNAP HQ2 camera. Stacks of 12 pictures were taken every 10 min with visible light and fluorescence. Best focus images were compiled and analyzed with the MetaMorph software.

Histological Procedures

For cryostat and paraplast sections, embryos were fixed, respectively, in 4% paraformaldehyde or Formoy's solution and processed as described in Pouget et al. (2006).

Immunohistology
Antibodies

Sections were stained with QCPN (developed by Carlson and Carlson), which recognizes all quail cell nuclei, and was obtained from the Developmental Studies Hybridoma Bank developed under the auspices of the NICHD and maintained by The University of Iowa, Department of Biological Sciences

(Iowa City, IA, USA); anti-α-smooth muscle actin (αSMA; Sigma-Aldrich, clone 1A4); anti-chicken CD45 antibody (HISC7; Cedi-Diagnostics B.V., the Netherlands); and anti-GFP (Roche Applied Science). Secondary goat anti-mouse (GAM) antibodies were used coupled to biotin, Horse Radish Peroxydase (Southern Biotechnology Associated), and Alexa Fluor 488 (Molecular Probes). Tyramide Signal Amplification Cyanin 3 (PerkinElmer) was used to increase the signal. Sections were counterstained with DAPI.

In Situ Hybridization on Sections
Hybridization was performed according to Minko et al. (2003) and Wilting et al. (1997).
RNA Probes
The chicken *cjagged1*, *cjagged2*, *notch2*, and *delta1* probes were gifts from Dr. R. Goitsuka, (Research Institute for Biological Sciences, Chiba, Japan.). Chicken *notch1* extracellular domain was from Dr. M. Marx (Institut Curie, Orsay, France). Chicken *dll4* was kindly provided by Dr. M. Scaal (Freiburg, Germany). Chicken *pu1* probe was from Dr. Z. Kherrouche (Institut de Biologie de Lille, France). Chicken *myb*, *runx1*, and *ve-cadherin* probes were obtained as described (Bollerot et al., 2005). Sense and antisense RNA probes were synthesized using r-UTP-Digoxygenin (Roche).

CFDA-SE Labeling
CFDA-SE (Invitrogen) was used to label the splanchnic mesoderm. A 10 mM CFDA-SE stock solution in DMSO (Sigma-Aldrich) was diluted in PBS and inoculated in ovo into the coelomic cavities at the cervical levels of 19–22 somite-stage embryos with a borosilicated glass capillary. Inoculated embryos were checked under a UV lamp and incubated for an additional 24 hr period.

Aorta and Cell Cultures
In Vitro Aorta Organotypic Culture
E9.5 mouse or E3 chicken aortas were dissected out and submitted to organotypic cultures on OP9 cells (Nakano et al., 1994) as previously described by Kumano et al. (2003). Briefly, aorta explants were seeded on OP9 stromal cells in RPMI 1640 (Invitrogen) with 10% fetal calf serum (FCS) supplemented with 50 ng/ml Stem Cell Factor and 5 ng/ml recombinant mouse Interleukin3 (PromoCell) with or without 50 μM DAPT (Sigma-Aldrich), and incubated at 37°C in 5%CO$_2$ for 7 days. Half of the medium was renewed at days 1 and 4 of culture.
HC Assays
After the 7 days of organotypic culture, aortas and OP9 cells were dissociated mechanically by pipetting and thereafter by collagenase I treatment for 30 min at 37°C. After centrifugation, cell pellets were resuspended in RPMI 1640 with 10% FCS and adherent cells allowed to attach on tissue culture plates for 40 min at 37°C. Nonadherent HCs were then recovered, counted, and submitted to methylcellulose CFC assay (10,000 cells plated) or D7-CAFC (2,000–20,000 cells plated), as previously described by Petit-Cocault et al. (2007). Cultures were maintained at 37°C, and colonies or CAFCs were scored at day 7.

Scanning Electron Microscopy
Avian embryos were fixed in 4% glutararaldehyde/1× PBS for 1 hr at RT. Embryos were included in 1% low melting point agarose (Invitrogen). Sections of 300 μm thick were obtained on a Leica VT1000S vibratome. Samples were postfixed in 1% OsO$_4$ in 2× PBS for 1 hr at RT. Samples were dehydrated in successive ethanol baths from 30% to 95% 10 min each and three baths in 100% ethanol. Samples were dried by hexamethyldisilazane (Sigma-Aldrich), vacuum desiccated overnight, mounted onto 12 mm SEM stubs (EM Sciences), and gold-palladium sputter coated. Coverslips were viewed on a Cambridge S220 scanning electron microscope at 12 kV and 15 mm working distance. Pictures were acquired with the Orion 6.60.4 software and colorized using Photoshop CS3.

Electroporation of DNA Constructs into the Endothelium of Dorsal Aorta in the Chicken Embryo
A total of 15 embryos ranging between 26 and 28 somite stage were used and processed as in Rosselló and Torres (2010). RBPJ-k reporter pTP1-Venus construct, kind gift from Dr. Okano, Tokyo, Japan (Kohyama et al., 2005;

Sato et al., 2008) was diluted in RNase-free water (2 μg/μl) alongside with the construct pECFP-N1 (BD Biosciences) (6:1 ratio). Electroporated embryos were incubated for an additional 24 hr period and checked under a UV lamp before collection.

FACS of ECs and HCs and Flow Cytometry Analysis
Chicken ECs were metabolically stained using inoculation of Alexa 488-coupled acetylated low-density lipoproteins into the heart of E2 or E3 embryos as described (Jaffredo et al., 1998). HCs were labeled at E3 using the chicken-specific anti-CD45 (HISC7)-coupled Phycoerythrin (PE) (SouthernBiotech, Birmingham, AL, USA; clone DT40).

E9 mouse ECs were isolated from their surface expression of CD31 (PECAM). E11.5 mouse ECs and HCs were sorted on the basis of, respectively, CD144$^+$ CD45$^-$ and CD144$^+$ CD45$^+$ as described. E11.5 mouse *Runx1$^{gfp/gfp}$* AGM regions (Lorsbach et al., 2004) were sorted into hemogenic endothelium, immature, and mature hematopoietic cluster cell fractions via FACS on a low-speed FACSVantage SE. Dead cells were excluded by 7-Amino-Actinomycin D (BD Biosciences), and populations were sorted based on expression of GFP, Alexa Fluor 647 anti-mouse CD144 (eBioscience), PE anti-mouse CD41, and APC-Cy7 Rat anti-mouse CD45 (BD Biosciences).

Cell staining of chick and mouse P-Sp cultures was done in PBS with 0.5% BSA using the following antibodies: allophycocyanin (APC)-coupled anti-chick or anti-mouse CD45 (Southern Biotech and BioLegend, respectively). For annexin V analysis, immunostained cells were resuspended in annexin V buffer and stained with fluorescein isothiocyanate (FITC)-annexin V (BioLegend) according to the manufacturer's guidelines. Dead cells were excluded by 7AAD (Beckman Coulter) staining. FACS analysis was performed on a LSRII flow cytometer (BD Biosciences).

REFERENCES

Azcoitia, V., Aracil, M., Martínez-A., C., and Torres, M. (2005). The homeodomain protein Meis1 is essential for definitive hematopoiesis and vascular patterning in the mouse embryo. Dev. Biol. *280*, 307–320.

Bee, T., Ashley, E.L., Bickley, S.R., Jarratt, A., Li, P.S., Sloane-Stanley, J., Göttgens, B., and de Bruijn, M.F. (2009). The mouse Runx1 +23 hematopoietic stem cell enhancer confers hematopoietic specificity to both Runx1 promoters. Blood *113*, 5121–5124.

Bertrand, J.Y., Giroux, S., Golub, R., Klaine, M., Jalil, A., Boucontet, L., Godin, I., and Cumano, A. (2005). Characterization of purified intraembryonic hematopoietic stem cells as a tool to define their site of origin. Proc. Natl. Acad. Sci. USA *102*, 134–139.

Bertrand, J.Y., Chi, N.C., Santoso, B., Teng, S., Stainier, D.Y., and Traver, D. (2010a). Haematopoietic stem cells derive directly from aortic endothelium during development. Nature *464*, 108–111.

Bertrand, J.Y., Cisson, J.L., Stachura, D.L., and Traver, D. (2010b). Notch signaling distinguishes 2 waves of definitive hematopoiesis in the zebrafish embryo. Blood *115*, 2777–2783.

Boisset, J.C., van Cappellen, W., Andrieu-Soler, C., Galjart, N., Dzierzak, E., and Robin, C. (2010). In vivo imaging of haematopoietic cells emerging from the mouse aortic endothelium. Nature *464*, 116–120.

Bollerot, K., Romero, S., Dunon, D., and Jaffredo, T. (2005). Core binding factor in the early avian embryo: cloning of Cbfbeta and combinatorial expression patterns with Runx1. Gene Expr. Patterns *6*, 29–39.

Burns, C.E., Traver, D., Mayhall, E., Shepard, J.L., and Zon, L.I. (2005). Hematopoietic stem cell fate is established by the Notch-Runx pathway. Genes Dev. *19*, 2331–2342.

Chapman, S.C., Collignon, J., Schoenwolf, G.C., and Lumsden, A. (2001). Improved method for chick whole-embryo culture using a filter paper carrier. Dev. Dyn. *220*, 284–289.

Chen, M.J., Yokomizo, T., Zeigler, B.M., Dzierzak, E., and Speck, N.A. (2009). Runx1 is required for the endothelial to haematopoietic cell transition but not thereafter. Nature *457*, 887–891.

Clements, W.K., Kim, A.D., Ong, K.G., Moore, J.C., Lawson, N.D., and Traver, D. (2011). A somitic Wnt16/Notch pathway specifies haematopoietic stem cells. Nature *474*, 220–224.

Cortés, F., Debacker, C., Péault, B., and Labastie, M.C. (1999). Differential expression of KDR/VEGFR-2 and CD34 during mesoderm development of the early human embryo. Mech. Dev. *83*, 161–164.

de Bruijn, M.F., Speck, N.A., Peeters, M.C., and Dzierzak, E. (2000). Definitive hematopoietic stem cells first develop within the major arterial regions of the mouse embryo. EMBO J. *19*, 2465–2474.

Dieterlen-Lièvre, F., Pouget, C., Bollérot, K., and Jaffredo, T. (2006). Are intra-aortic hemopoietic cells derived from endothelial cells during ontogeny? Trends Cardiovasc. Med. *16*, 128–139.

Durand, C., Robin, C., Bollerot, K., Baron, M.H., Ottersbach, K., and Dzierzak, E. (2007). Embryonic stromal clones reveal developmental regulators of definitive hematopoietic stem cells. Proc. Natl. Acad. Sci. USA *104*, 20838–20843.

Dzierzak, E., and Speck, N.A. (2008). Of lineage and legacy: the development of mammalian hematopoietic stem cells. Nat. Immunol. *9*, 129–136.

Eilken, H.M., Nishikawa, S., and Schroeder, T. (2009). Continuous single-cell imaging of blood generation from haemogenic endothelium. Nature *457*, 896–900.

Galmiche, M.C., Koteliansky, V.E., Brière, J., Hervé, P., and Charbord, P. (1993). Stromal cells from human long-term marrow cultures are mesenchymal cells that differentiate following a vascular smooth muscle differentiation pathway. Blood *82*, 66–76.

Hadland, B.K., Huppert, S.S., Kanungo, J., Xue, Y., Jiang, R., Gridley, T., Conlon, R.A., Cheng, A.M., Kopan, R., and Longmore, G.D. (2004). A requirement for Notch1 distinguishes 2 phases of definitive hematopoiesis during development. Blood *104*, 3097–3105.

Hernandez-Munain, C., and Krangel, M.S. (1994). Regulation of the T-cell receptor delta enhancer by functional cooperation between c-Myb and core-binding factors. Mol. Cell. Biol. *14*, 473–483.

Huang, G., Zhang, P., Hirai, H., Elf, S., Yan, X., Chen, Z., Koschmieder, S., Okuno, Y., Dayaram, T., Growney, J.D., et al. (2008). PU.1 is a major downstream target of AML1 (RUNX1) in adult mouse hematopoiesis. Nat. Genet. *40*, 51–60.

Jaffredo, T., Gautier, R., Eichmann, A., and Dieterlen-Lièvre, F. (1998). Intraaortic hemopoietic cells are derived from endothelial cells during ontogeny. Development *125*, 4575–4583.

Jaffredo, T., Bollerot, K., Sugiyama, D., Gautier, R., and Drevon, C. (2005). Tracing the hemangioblast during embryogenesis: developmental relationships between endothelial and hematopoietic cells. Int. J. Dev. Biol. *49*, 269–277.

Jaffredo, T., Richard, C., Pouget, C., Teillet, M.A., Bollérot, K., Gautier, R., and Drevon, C. (2010). Aortic remodelling during hemogenesis: is the chicken paradigm unique? Int. J. Dev. Biol. *54*, 1045–1054.

Kimura, W., Yasugi, S., Stern, C.D., and Fukuda, K. (2006). Fate and plasticity of the endoderm in the early chick embryo. Dev. Biol. *289*, 283–295.

Kissa, K., and Herbomel, P. (2010). Blood stem cells emerge from aortic endothelium by a novel type of cell transition. Nature *464*, 112–115.

Kohyama, J., Tokunaga, A., Fujita, Y., Miyoshi, H., Nagai, T., Miyawaki, A., Nakao, K., Matsuzaki, Y., and Okano, H. (2005). Visualization of spatiotemporal activation of Notch signaling: live monitoring and significance in neural development. Dev. Biol. *286*, 311–325.

Kumano, K., Chiba, S., Kunisato, A., Sata, M., Saito, T., Nakagami-Yamaguchi, E., Yamaguchi, T., Masuda, S., Shimizu, K., Takahashi, T., et al. (2003). Notch1 but not Notch2 is essential for generating hematopoietic stem cells from endothelial cells. Immunity *18*, 699–711.

Lam, E.Y., Hall, C.J., Crosier, P.S., Crosier, K.E., and Flores, M.V. (2010). Live imaging of Runx1 expression in the dorsal aorta tracks the emergence of blood progenitors from endothelial cells. Blood *116*, 909–914.

Lancrin, C., Sroczynska, P., Stephenson, C., Allen, T., Kouskoff, V., and Lacaud, G. (2009). The haemangioblast generates haematopoietic cells through a haemogenic endothelium stage. Nature *457*, 892–895.

Lorsbach, R.B., Moore, J., Ang, S.O., Sun, W., Lenny, N., and Downing, J.R. (2004). Role of RUNX1 in adult hematopoiesis: analysis of RUNX1-IRES-GFP knock-in mice reveals differential lineage expression. Blood *103*, 2522–2529.

Marshall, C.J., Moore, R.L., Thorogood, P., Brickell, P.M., Kinnon, C., and Thrasher, A.J. (1999). Detailed characterization of the human aorta-gonad-mesonephros region reveals morphological polarity resembling a hematopoietic stromal layer. Dev. Dyn. *215*, 139–147.

Marshall, C.J., Kinnon, C., and Thrasher, A.J. (2000). Polarized expression of bone morphogenetic protein-4 in the human aorta-gonad-mesonephros region. Blood *96*, 1591–1593.

Minko, K., Bollerot, K., Drevon, C., Hallais, M.F., and Jaffredo, T. (2003). From mesoderm to blood islands: patterns of key molecules during yolk sac erythropoiesis. Gene Expr. Patterns *3*, 261–272.

Nakano, T., Kodama, H., and Honjo, T. (1994). Generation of lymphohematopoietic cells from embryonic stem cells in culture. Science *265*, 1098–1101.

Ng, C.E., Yokomizo, T., Yamashita, N., Cirovic, B., Jin, H., Wen, Z., Ito, Y., and Osato, M. (2010). A Runx1 intronic enhancer marks hemogenic endothelial cells and hematopoietic stem cells. Stem Cells *28*, 1869–1881.

North, T., Gu, T.L., Stacy, T., Wang, Q., Howard, L., Binder, M., Marín-Padilla, M., and Speck, N.A. (1999). Cbfa2 is required for the formation of intra-aortic hematopoietic clusters. Development *126*, 2563–2575.

North, T.E., de Bruijn, M.F., Stacy, T., Talebian, L., Lind, E., Robin, C., Binder, M., Dzierzak, E., and Speck, N.A. (2002). Runx1 expression marks long-term repopulating hematopoietic stem cells in the midgestation mouse embryo. Immunity *16*, 661–672.

Nottingham, W.T., Jarratt, A., Burgess, M., Speck, C.L., Cheng, J.F., Prabhakar, S., Rubin, E.M., Li, P.S., Sloane-Stanley, J., Kong-A-San, J., and de Bruijn, M.F. (2007). Runx1-mediated hematopoietic stem-cell emergence is controlled by a Gata/Ets/SCL-regulated enhancer. Blood *110*, 4188–4197.

Oberlin, E., Tavian, M., Blazsek, I., and Péault, B. (2002). Blood-forming potential of vascular endothelium in the human embryo. Development *129*, 4147–4157.

Oostendorp, R.A., Harvey, K.N., Kusadasi, N., de Bruijn, M.F., Saris, C., Ploemacher, R.E., Medvinsky, A.L., and Dzierzak, E.A. (2002). Stromal cell lines from mouse aorta-gonads-mesonephros subregions are potent supporters of hematopoietic stem cell activity. Blood *99*, 1183–1189.

Pardanaud, L., and Dieterlen-Lièvre, F. (1999). Manipulation of the angiopoietic/hemangiopoietic commitment in the avian embryo. Development *126*, 617–627.

Pardanaud, L., Luton, D., Prigent, M., Bourcheix, L.-M., Catala, M., and Dieterlen-Lievre, F. (1996). Two distinct endothelial lineages in ontogeny, one of them related to hemopoiesis. Development *122*, 1363–1371.

Peeters, M., Ottersbach, K., Bollerot, K., Orelio, C., de Bruijn, M., Wijgerde, M., and Dzierzak, E. (2009). Ventral embryonic tissues and Hedgehog proteins induce early AGM hematopoietic stem cell development. Development *136*, 2613–2621.

Petit-Cocault, L., Volle-Challier, C., Fleury, M., Péault, B., and Souyri, M. (2007). Dual role of Mpl receptor during the establishment of definitive hematopoiesis. Development *134*, 3031–3040.

Pimanda, J.E., Ottersbach, K., Knezevic, K., Kinston, S., Chan, W.Y., Wilson, N.K., Landry, J.R., Wood, A.D., Kolb-Kokocinski, A., Green, A.R., et al. (2007). Gata2, Fli1, and Scl form a recursively wired gene-regulatory circuit during early hematopoietic development. Proc. Natl. Acad. Sci. USA *104*, 17692–17697.

Pouget, C., Gautier, R., Teillet, M.A., and Jaffredo, T. (2006). Somite-derived cells replace ventral aortic hemangioblasts and provide aortic smooth muscle cells of the trunk. Development *133*, 1013–1022.

Robert-Moreno, A., Espinosa, L., de la Pompa, J.L., and Bigas, A. (2005). RBPjkappa-dependent Notch function regulates Gata2 and is essential for the formation of intra-embryonic hematopoietic cells. Development *132*, 1117–1126.

Robert-Moreno, A., Guiu, J., Ruiz-Herguido, C., López, M.E., Inglés-Esteve, J., Riera, L., Tipping, A., Enver, T., Dzierzak, E., Gridley, T., et al. (2008). Impaired embryonic haematopoiesis yet normal arterial development in the absence of the Notch ligand Jagged1. EMBO J. *27*, 1886–1895.

Rosselló, C.A., and Torres, M. (2010). Gene transfer by electroporation into hemogenic endothelium in the avian embryo. Dev. Dyn. *239*, 1748–1754.

Rowlinson, J.M., and Gering, M. (2010). Hey2 acts upstream of Notch in hematopoietic stem cell specification in zebrafish embryos. Blood *116*, 2046–2056.

Rybtsov, S., Sobiesiak, M., Taoudi, S., Souilhol, C., Senserrich, J., Liakhovitskaia, A., Ivanovs, A., Frampton, J., Zhao, S., and Medvinsky, A.

(2011). Hierarchical organization and early hematopoietic specification of the developing HSC lineage in the AGM region. J. Exp. Med. *208*, 1305–1315.

Sato, Y., Watanabe, T., Saito, D., Takahashi, T., Yoshida, S., Kohyama, J., Ohata, E., Okano, H., and Takahashi, Y. (2008). Notch mediates the segmental specification of angioblasts in somites and their directed migration toward the dorsal aorta in avian embryos. Dev. Cell *14*, 890–901.

Taoudi, S., and Medvinsky, A. (2007). Functional identification of the hematopoietic stem cell niche in the ventral domain of the embryonic dorsal aorta. Proc. Natl. Acad. Sci. USA *104*, 9399–9403.

Wasteson, P., Johansson, B.R., Jukkola, T., Breuer, S., Akyürek, L.M., Partanen, J., and Lindahl, P. (2008). Developmental origin of smooth muscle cells in the descending aorta in mice. Development *135*, 1823–1832.

Wiegreffe, C., Christ, B., Huang, R., and Scaal, M. (2009). Remodeling of aortic smooth muscle during avian embryonic development. Dev. Dyn. *238*, 624–631.

Wilkinson, R.N., Pouget, C., Gering, M., Russell, A.J., Davies, S.G., Kimelman, D., and Patient, R. (2009). Hedgehog and Bmp polarize hematopoietic stem cell emergence in the zebrafish dorsal aorta. Dev. Cell *16*, 909–916.

Wilting, J., Eichmann, A., and Christ, B. (1997). Expression of the avian VEGF receptor homologues Quek1 and Quek2 in blood-vascular and lymphatic endothelial and non-endothelial cells during quail embryonic development. Cell Tissue Res. *288*, 207–223.

Yokomizo, T., and Dzierzak, E. (2010). Three-dimensional cartography of hematopoietic clusters in the vasculature of whole mouse embryos. Development *137*, 3651–3661.

Zovein, A.C., Hofmann, J.J., Lynch, M., French, W.J., Turlo, K.A., Yang, Y., Becker, M.S., Zanetta, L., Dejana, E., Gasson, J.C., et al. (2008). Fate tracing reveals the endothelial origin of hematopoietic stem cells. Cell Stem Cell *3*, 625–636.